ORIGINAL RESEARCH

Tract-Based Analysis of Callosal, Projection, and Association Pathways in Pediatric Patients with Multiple Sclerosis: A Preliminary Study

M.S. Vishwas
T. Chitnis
R. Pienaar
B.C. Healy
P.E. Grant

BACKGROUND AND PURPOSE: Region-of-interest (ROI) and tract-based diffusion tensor imaging (DTI) analyses have detected increased apparent diffusion coefficients (ADCs) and decreased fractional anisotropy (FA) in callosal and projection systems of adult patients with multiple sclerosis (MS). We explored whether similar changes occur in pediatric patients with MS, assessing 3 major white matter pathways (interhemispheric, projection, and intrahemispheric) in both visibly involved and normal-appearing white matter (NAWM).

MATERIALS AND METHODS: DTI datasets from 10 patients with established pediatric MS and 10 age-sex-, and imaging technique–matched controls were analyzed. Tracts were reconstructed by using a fiber assignment by continuous tracking algorithm with a diffusion-weighted imaging mask and a 35° angular threshold. Tracts were selected by using standard ROI placements on color FA maps cross-referenced to $b = 0$ T2-weighted images for studying white matter pathways. Ten identical ROIs were placed in NAWM on $b = 0$ T2-weighted images to ensure that both ROIs and resulting tracts passed through NAWM.

RESULTS: In pediatric MS, all tracts had higher mean ADC values ($P = .002$ to $P < .04$) and lower mean FA ($P = .009$ to $P < .02$) than those in healthy controls. Even when the tracts were confined to NAWM, the mean ADC was higher ($P < .004$ to $P < .05$) and the mean FA was lower ($P = .002$ to $P < .02$). T2 lesion burden correlated with tract-based mean ADC. ROI mean ADC increased, and both tract and ROI mean FA decreased with increasing T2 lesion burden, however with a statistically nonsignificant correlation.

CONCLUSIONS: Increased mean ADC and decreased mean FA occur in all 3 major white matter pathways, both in visibly involved white matter and NAWM in pediatric MS.

PEDIATRICS

ORIGINAL RESEARCH

Multiple sclerosis (MS) generally begins in the second-to-third decade of life; however, it is increasingly recognized that MS occurs in children.[1] It is estimated that up to 10.5% of all cases of MS may have disease onset before 18 years of age.[1-4] Little is known about the pathogenesis of pediatric MS and the similarities and differences compared with adult-onset MS. Children with MS appear to experience a more inflammatory course of disease and accrue physical disability more slowly than adults; however, they have significant cognitive dysfunctions.[2,4-7]

The pathology of MS is a result of both focal damage and distal processes, including retrograde degeneration, the latter of which can cause diffuse alterations in tissue structure in normal-appearing white matter (NAWM),[8,9] which are generally not apparent on conventional MR imaging. Such changes have been associated with more progressive and irreversible disability.[9,10] The location and extent of focal and diffuse tissue damage in children with MS is unknown. This is particularly important in understanding the underlying pathogenesis, the major functional systems involved, and factors related to the accrual of long-term clinical and cognitive disabilities.[1]

MR imaging, in particular conventional T2-weighted imaging, is the best noninvasive reflection of the pathologic processes occurring in MS. MR imaging facilitates correlation with clinical disease and categorization into subtypes.[11] However assessing disease burden on the basis of T2 lesion load alone has its limitations, due in part to the lack of specificity and spatial orientation and the inability to identify diffuse changes that occur in MS.

Diffusion tensor imaging (DTI) quantifies the diffusive motion of water molecules. Diffusion of water molecules along the white matter fibers is relatively free; however, it is restricted perpendicularly by the myelin. Pathologic processes affecting the brain can modify water molecule diffusion. The quantitative parameters of DTI include apparent diffusion coefficient (ADC) and an anisotropy measure such as fractional anisotropy (FA).[12-14] ADC is the measure of average water molecular motion independent of directionality. The microscopic features, such as cellular size and fraction of extracellular space, affect ADC values.[13,14] FA is a quantitative measure of deviation from isotropy and reflects the degree of alignment of cellular structures and tissue coherence.[13-15] Brain white matter has an oriented microstructure due to the presence of discrete white matter tracts that give rise to regions with aligned axons, resulting in high anisotropy. MS lesions and NAWM of adult patients with MS have been shown to have

Received April 6, 2009; accepted after revision May 22.

From the Athinoula A. Martinos Center for Biomedical Imaging (M.S.V., R.P., E.P.G.), Massachusetts General Hospital, Harvard Medical School, Boston, Massachusetts; Partners Pediatric Multiple Sclerosis Center (T.C.), Massachusetts General Hospital for Children, Harvard Medical School, Boston, Massachusetts; Biostatistics Center (B.C.H.), Massachusetts General Hospital, Boston, Massachusetts; and Department of Neurology (T.C.), Brigham and Women's Hospital, Harvard Medical School, Boston, Massachusetts.

We thank Ruopeng Wang and Van J. Wedeen of Athinoula A. Martinos Center for Biomedical Imaging, the Department of Radiology, Massachusetts General Hospital; and the National Multiple Sclerosis Society for funding support (Pediatric MS Centers of Excellence award to T.C).

Please address correspondence to P. Ellen Grant, MD, Athinoula A. Martinos Center for Biomedical Imaging, Building 149, 13th St, Ste 2301, Charlestown, MA 02129; e-mail: ellen@nmr.mgh.harvard.edu

DOI 10.3174/ajnr.A1776

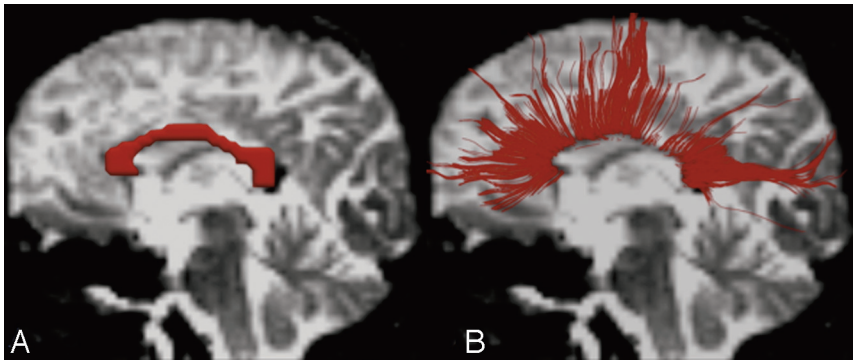

Fig 1. Regions of interest (ROIs) of the corpus callosum (CC) and interhemispheric fibers. *A,* A single ROI is placed in the midline CC in the midsaggital plane for studying callosal fibers on the background of a $b = 0$ T2-weighted image.[29] The ROI is red. *B,* Left lateral view of a 3D reconstruction of callosal fibers passing through the genu, body, and splenium of the CC in the background of a $b = 0$ T2-weighted image.

increased ADC and decreased FA.[15-18] The alteration in these DTI measures is presumed to reflect the decreased white matter tract integrity and axonal damage both locally and distally.

Diffusion tractography is an extension of DTI, in which the directional information of water molecule diffusion is used to generate virtual 3D white matter tracts.[19] Tractography enables white matter to be parcellated into white matter pathways that have functional specificity and, therefore, enables assessment of disease processes in terms of functional systems. Studies in the adult MS population have found callosal and corticospinal tracts involved more frequently than in healthy controls,[20-23] with involvement correlating with cognitive dysfunction and motor disabilities, respectively.[21,23-25]

MS in children and adolescents is an increasingly recognized disorder; however, little is known about its pathophysiology and MR imaging characteristics. To date, there are only 2 studies that have attempted to quantify the extent of brain and cervical cord damage in pediatric MS by using DTI and magnetization transfer ratio.[26,27] Mezzapesa et al[26] showed only a modest increase of mean ADC in NAWM compared with that in healthy controls, in contrast to what has been reported in adult patients with MS.[18,23] Tortorella et al[27] showed increased ADC and decreased FA in the NAWM of pediatric patients with MS compared with healthy controls. Neither of these studies used ROI and tract-based analyses. In our study, we have investigated the extent of diffusion abnormalities on 3 major white matter pathways (interhemispheric, projection, and intrahemispheric) in pediatric patients with MS to determine their involvement with ADC and FA measures. In addition, we analyzed the diffusion parameters in NAWM and the fibers passing through it, hypothesizing that the white matter containing lesioned and nonlesioned pathways and the NAWM not containing lesioned pathways are both affected.

Materials and Methods

Recruitment of Patients

A retrospective search of the Partners Pediatric MS Center clinical data base from 2004 to 2008 yielded 10 patients younger than of 18 years of age who met our inclusion criteria of a diagnosis of relapsing-remitting multiple sclerosis (RRMS) based on the diagnostic criteria proposed by International Pediatric MS Study Group,[6] with ≥1 MR image with DTI sequences performed on Sonata and Avanto (Siemens, Erlangen, Germany) scanners at Massachusetts General Hospital (MGH). The images of 10 age-, sex-, MR imaging scanner–matched, and imaging technique–matched normative controls were obtained from the MGH clinical data base as a comparative cohort. Normative controls were children with headache as the presenting symptom, normal findings on clinical examination, and grossly normal findings on brain MR imaging studies. Approval for this work was obtained from the Partners Internal Review Board on Human Studies.

MR Imaging Acquisition

All scanning was performed on 1.5T Avanto and Sonata scanners (Siemens) at MGH. All patients had conventional proton attenuation–weighted and T2-weighted images (TR/TE = 3350–7260/97–109 ms and 4- to 5-mm-thick sections) as well as DTI. DTI sequences had the following specifications: 8 patients and 8 controls (one–five $b = 0$, TR/TE = 3000–5000/83–97 ms, 23 contiguous 6-mm-thick sections, voxel size = 1.72 × 1.72 × 6 and 12–30 gradient directions at $b = 1000$ s/mm^2), 1 patient and 1 control (five $b = 0$, 52 contiguous 3-mm-thick sections, TR/TE = 6570/87 ms, voxel size = 2.29 × 2.29 × 3 and 29 gradient directions at $b = 1000$ s/mm^2), and 1 patient and 1 control (5 $b = 0$, TR/TE = 7580/87 ms, 60 contiguous 2.2-mm-thick sections, voxel size = 2.2 × 2.2 × 2.2 and 29 gradient directions at $b = 1000$ s/mm^2). The images were transferred to a computer workstation for tractography reconstruction. All 10 control MR images were matched for the scanner subtype, section thickness, and gradient directions.

Postprocessing and Analysis of DTIs

Batch processing was facilitated by using a custom-made postprocessing stream to operate directly on the DICOM images as input. Diffusion Toolkit (www.trackvis.org, Diffusion Toolkit, Version 0.4.2) and the diffusion-weighted imaging (DWI) mask–generated voxel-based tensor data were used for track reconstruction. TrackVis (www.trackvis.org, TrackVis, Version 0.4.2) was used for ROI and fiber-track data analysis. Tracts were reconstructed by using a fiber assignment by continuous tracking (FACT)[28] algorithm and an angular threshold of 35°. We used a DWI mask to remove CSF but did not use an FA threshold for tract reconstruction, because the standard FA threshold of 0.2 would drop out tracts passing through some MS lesions and bias our results. To create the fiber systems of interest, we took the starting point

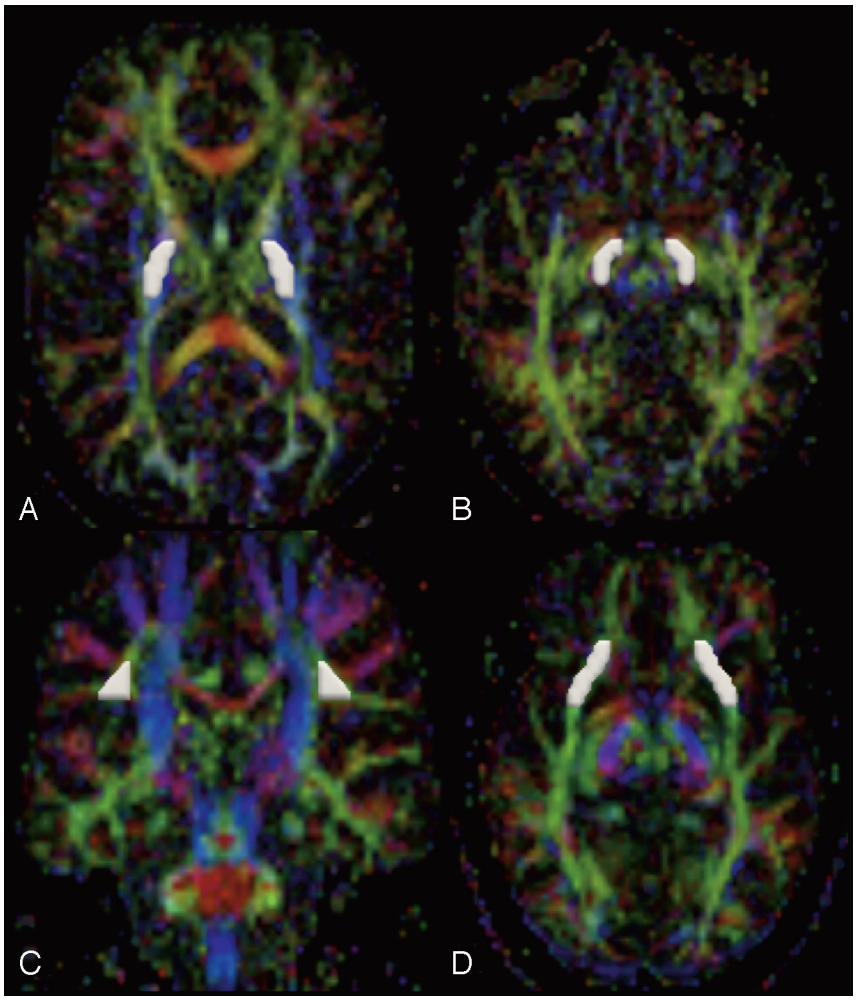

Fig 2. ROIs for the projection fibers and long association fibers (LAF) placed on color fractional anisotropy (FA) images. *A* and *B*, A 2-ROI approach is used for the projection fibers. One ROI is placed in the posterior limb of the internal capsule (PLIC) and a second ROI is placed in the cerebral peduncle (CP) on the axial plane at the level of the midbrain to generate the projection fibers.[29] *C* and *D*, A 2-ROI approach is used for LAF (superior longitudinal fasciculus [SLF], inferior fronto-occipital fasciculus [IFOF], and uncinate fasciculus [UF]). One ROI is placed in the coronal plane for the SLF, lateral to the corona radiata,[36,42] and a second ROI, on the axial plane at the level of anterior margin of external capsule, where the IFOF and UF pass close to each other.[30] All the regions of interest are white.

manually by defining a ROI by referring to standard color FA[29] and tractography atlases.[30,31]

Catani and Thiebaut de Schotten[31] have reported that manually defined ROI placement has advantages over ROI delineation by automatic application of normalized cortical or subcortical masks in studying desired pathways. The tracts resulting from our analysis were visually assessed to ensure anatomic accuracy on the basis of these previously published tractography atlases and to confirm that the absence of an FA threshold did not result in spurious tracts. All the ROIs were placed on the color FA maps cross-referenced with $b = 0$ T2-weighted images for accurate anatomic placement of the ROIs. The $b = 0$ T2-weighted images were used because they are part of the diffusion tensor dataset acquisition; therefore, the $b = 0$ images are naturally aligned with and have distortions similar to the diffusion tensor data. Also because the diffusion data are a lower resolution than the conventional images, partial volume averaging is going to occur in the diffusion data. Therefore, using a higher resolution conventional T2 to draw ROIs would not improve the accuracy of the measured ADC or FA values in these lesions.

A single ROI was placed in the entire corpus callosum (CC) in the mid-saggital plane for the inter-hemispheric fiber pathway (Fig 1*A*),[29,31,32] A two ROI approach was used for studying projection and long association fibers (LAF). One ROI was placed in the posterior limb of the internal capsule (PLIC) (Fig. 2*A*) and a second ROI was placed in the cerebral peduncle (CP) (Fig. 2*B*) on the axial plane at the level of the midbrain to generate the projection fibers.[29,31] For LAF, which include the superior longitudinal fasciculus (SLF), inferior fronto-occipital fasciculus (IFOF), and uncinate fasciculus (UF) (Fig 2*C*, -*D*),[30] one ROI is placed in the coronal plane for the SLF, lateral to the corona radiata,[36,42] and a second ROI, on the axial plane at the level of anterior margin of eternal capsule, where the IFOF and UF pass close to each other. The tracts intersecting the single ROI (Fig. 1*B*) or both ROIs (Fig 3*A* and 3*B*) were constructed allowing tract-based measures.

For NAWM, 10 identical ROIs were placed on color FA maps with cross-referencing to $b = 0$ T2-weighted images (Fig 4*A*–*D*) to ensure that ROIs were placed in NAWM. These ROIs were placed in the genu and splenium of the CC (Fig 4*A*), 2 ROIs each in the PLIC (Fig 4*A*) and CP (Fig 4*B*). For association pathways in NAWM, 2 ROIs were placed in the axial plane above the body of the CC lateral to the corona radiata to

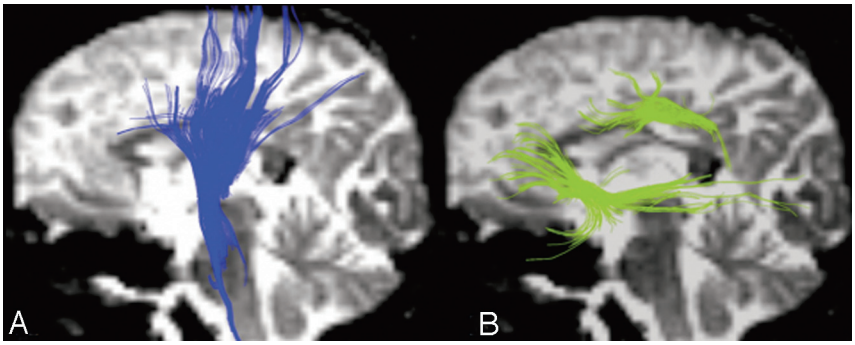

Fig 3. Left lateral view of the 3D reconstruction of projection fibers and LAF on the background of a $b = 0$ T2-weighted image. *A*, Projection fibers. *B*, LAF (SLF, IFOF, and UF) pathway.

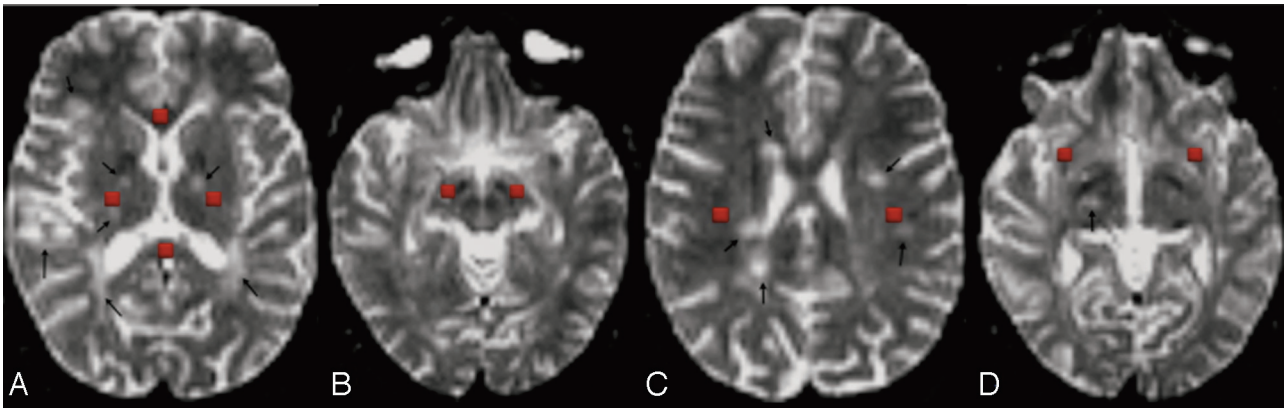

Fig 4. Regions of interest in the NAWM are placed on $b = 0$ T2-weighted images. *A*, One ROI is placed in the genu of the CC and one, in the splenium of the CC; and bilateral ROIs are placed in the PLIC. *B*, Bilateral ROIs are placed in the CP at the level of the midbrain. *C*, Bilateral ROIs for the SLF are placed in the axial plane, one section above the body of the CC lateral to the corona radiata. *D*, Bilateral ROIs are placed at the level of the anterior margin of the external capsule for the IFOF and UF. All the ROIs are red.

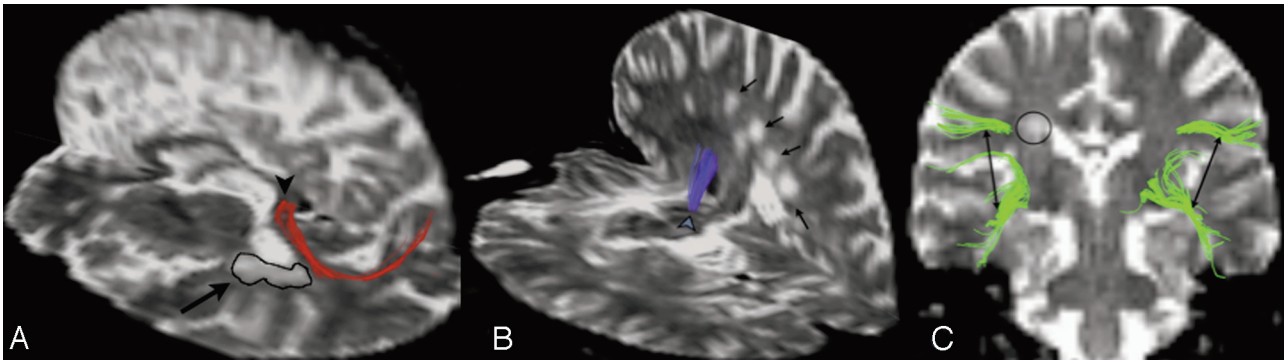

Fig 5. Callosal, projection, and association fibers passing through NAWM. *A*, Callosal fibers from the splenium of the CC passing through NAWM on the background of axial and sagittal planes of $b = 0$ T2-weighted images. A black arrow points to the T2 lesion on the axial plane, and the arrowhead points to the fibers from the splenium of the CC passing through NAWM. *B*, Projection fibers pass through NAWM in the background of the axial and sagittal planes of $b = 0$ T2-weighted images. Black arrows point to the T2 lesions, and the arrowhead points to the projection fibers passing through NAWM. *C*, The T2 lesion is encircled, and the arrows point to the association fibers passing through NAWM.

segment SLF (Fig 4*C*) and 2 ROIs, in the region at the level of anterior floor of the external capsule to segments IFOF and UF (Fig 4*D*). Tracts intersecting these ROIs were constructed. Any portion of the resulting tracts passing through regions of abnormal T2 signal intensity on $b = 0$ T2-weighted images were excluded (Fig 5*A–C*). ADC and FA images were loaded into TrackVis, and the mean ADC and FA in the specific ROIs and in the resulting tracts were recorded. All the ROIs were placed by a physician trained in tractography under the supervision of an experienced pediatric-neuroradiologist and a neurologist.

Statistical Analysis

A Wilcoxon signed rank test was used to compare the patients and the matched controls in terms of ROI mean ADC and mean FA as well as tract mean ADC and mean FA. The Spearman correlation coefficient was used to compare the number of lesions and NAWM ADC and FA measures. Given the exploratory nature of the study, no correction for multiple comparisons was completed. The data analysis for this article was generated by using the SAS System for Windows software, Version 9.1 (SAS Institute Inc, Cary, North Carolina)

Table 1: ROI and tract-based mean ADC and mean FA values of white matter pathways

	CC	PLIC	CP	LAF
ROI mean ADC $\times 10^{-3}$ mm^2/s				
Patients	1.11 ± 0.13	0.73 ± 0.02	0.88 ± 0.10	0.84 ± 0.07
Controls	0.89 ± 0.03	0.70 ± 0.03	0.76 ± 0.05	0.76 ± 0.02
P value	0.0020[a]	0.021[a]	0.020[a]	0.0059[a]
ROI mean FA				
Patients	0.53 ± 0.06	0.62 ± 0.02	0.65 ± 0.06	0.39 ± 0.04
Controls	0.63 ± 0.06	0.67 ± 0.03	0.69 ± 0.04	0.44 ± 0.02
P value	.0039[a]	.0039[a]	.13	.037[a]
Tract mean ADC $\times 10^{-3}$ mm^2/s				
Patients	0.97 ± 0.10	0.76 ± 0.04	0.81 ± 0.06	0.85 ± 0.06
Controls	0.86 ± 0.06	0.71 ± 0.03	0.73 ± 0.02	0.75 ± 0.02
P value	.037[a]	.0059[a]	.0020[a]	.0020[a]
Tract mean FA				
Patients	0.55 ± 0.06	0.56 v 0.03	0.58 ± 0.04	0.42 ± 0.04
Controls	0.62 ± 0.03	0.59 ± 0.02	0.62 ± 0.03	0.48 ± 0.02
P value	.0098[a]	.0098[a]	.0039[a]	.0098[a]

Note:—ROI indicates region of interest; CC, corpus callosum; PLIC, posterior limb of internal capsule; CP, cerebral peduncle; LAF, long association fibers; ADC, apparent diffusion coefficient; FA, fractional anisotropy.
[a] Statistically significant.

Lesion Burden on T2-Weighted Images

The total number of lesions in the CC and entire brain were counted and categorized on the basis of their size, ranging from 0 to 5 mm, 6 to 10 mm, 11 to 20 mm, and >20 mm for a comparative measure of disease severity.

Results

All patients had a diagnosis of RRMS. The mean age at the onset of disease was 15.25 years (range, 13.7–17.7 years); and at the time of the DTI acquisition, the mean age was 16.6 years (range, 15.1 to 18 years). There were 2 males and 8 females in our cohort. Mean disease duration was 1.67 years, and the mean treatment duration was 1.23 years, ranging from 1 month to 3.8 years. Seven of 10 patients were on beta-interferon, 1 patient was on glatiramer acetate (Copaxone), 1 patient was treated with multiple drugs (daclizumab, beta-interferon-1a, and methylprednisolone), and 1 patient was treated only with steroids. No patients received intravenous steroids within 30 days of MR imaging. The median Expanded Disability Status Scale score was 1.0 and ranged from 0 to 2. The mean age of the healthy controls was 16.68 years (range, 15.1–18.0 years).

ROI and Tract-Based Measures Including Involved White Matter

The mean ADC in the CC ROI was significantly elevated (P = .0020) (Table 1) as was the mean ADC in the ROIs for LAF (P = .0059), PLIC (P = .021), and CP (P = .020) when compared with normative controls. The mean FA in the CC region of interest was significantly reduced (P = .0039), as was the mean FA in the ROIs for the PLIC (P = .0039) and LAF (P = .027) compared with that in normative controls. The mean FA in the CP ROI (P = .13) was not significantly different compared with that in normative controls.

No spurious tracts resulted from the use of a DWI mask and from the use of no FA threshold. Tract-based mean ADC values were significantly increased in all tract systems (Table 1): LAF (P = .002), projection fibers (P = .0059 and P = .002), and callosal fibers (P = .037) compared with those in normative controls. A significant decrease was seen in the mean FA values along all tract systems studied: callosal fibers (P = .0098), LAF (P = .0098), and projection fibers (P = .0098 and P = .0039) compared with those in healthy controls.

ROI and Tract-Based Measures in NAWM

ROI mean ADCs in NAWM of the genu (P = .002) and splenium (P = .0039) of the CC; PLIC (P = .0098), CP (P = .037); and anatomic regions of association fibers, SLF (P = .014), and IFOF and UF (P = .002), were significantly higher than those in normative controls (Table 2). ROI mean FA of the splenium (P = .0059) of the CC, SLF (P = .0039), and IFOF and UF (P = .018) were significantly lower than those in normative controls. The mean FA in the ROIs for the genu of the CC (P = .28), PLIC (P = .25), and CP (P = .19) was not significantly different when compared with that in normative controls.

No spurious tracts resulted from the use of a DWI mask and from the use of no FA threshold. Tract-based mean ADC was significantly increased in all fibers passing through the ROIs of NAWM (Table 2): callosal fibers in the genu (P = .041) and splenium of the CC (P = .049); projection fibers in the PLIC (P = .0098) and CP (P = .0098); association fibers, SLF (P = .0039), IFOF and UF (P = .002); and aggregates of all the tracts passing through NAWM (P = .0098). Tract-based mean FA values were significantly decreased along callosal fibers passing through NAWM of the splenium of the CC (P = .002); projection fibers in the PLIC (P = .0098) and CP (P = .016); LAF: SLF (P = .0098), IFOF and UF (P = .014); and aggregates of all the tracts passing through NAWM (P = .002).

Lesion Count and Size

The total number of lesions counted on proton attenuation and T2-weighted images in the brain as well as in the CC was used for a comparative measure of disease severity. The mean total number of lesions in the CC and total brain was 0.8 and 54.6, respectively. The mean size of the lesions in the corpus callosum ranged from 3.8 to 5.4 mm, and the lesions in the entire brain ranged from 2 to 50 mm. Two patients had lesions in the CC, 1 patient had a confluent lesion, and 7 patients did not have any lesions in the CC.

Table 2: ROI and tract-based mean ADC and mean FA values of NAWM

	Controls	Patients	*P* Value
Region 1: genu of CC			
ROI mean ADC	0.77 ± 0.03	0.91 ± 0.14	.002[a]
ROI mean FA	0.80 ± 0.09	0.73 ± 0.10	.28
Tract mean ADC	0.78 ± 0.03	0.87 ± 0.10	.041[a]
Tract mean FA	0.62 ± 0.04	0.57 ± 0.06	.16
Region 2: Splenium of CC			
ROI mean ADC	0.74 ± 0.04	0.88 ± 0.11	.0039[a]
ROI mean FA	0.86 ± 0.05	0.78 ± 0.05	.0059[a]
Tract mean ADC	0.79 ± 0.05	0.85 ± 0.07	.049[a]
Tract mean FA	0.72 ± 0.03	0.66 ± 0.04	.002[a]
Region 3: PLIC			
ROI mean ADC	0.69 ± 0.03	0.72 ± 0.02	.0098[a]
ROI mean FA	0.69 ± 0.05	0.66 ± 0.03	.25
Tract mean ADC	0.71 ± 0.03	0.75 ± 0.04	.0098[a]
Tract mean FA	0.61 ± 0.03	0.57 ± 0.03	.0098[a]
Region 4: CP			
ROI mean ADC	0.71 ± 0.03	0.78 ± 0.05	.037[a]
ROI mean FA	0.73 ± 0.05	0.69 ± 0.04	.19
Tract mean ADC	0.72 ± 0.02	0.78 ± 0.04	.0098[a]
Tract mean FA	0.63 ± 0.03	0.60 ± 0.03	.016[a]
Region 5: Anatomic region for SLF			
ROI mean ADC	0.71 ± 0.03	0.74 ± 0.04	.014[a]
ROI mean FA	0.60 ± 0.06	0.47 ± 0.07	.0039[a]
Tract mean ADC	0.72 ± 0.03	0.79 ± 0.07	.0039[a]
Tract mean FA	0.54 ± .04	0.45 ± 0.05	.0098[a]
Region 6: Anatomic region for IFOF and UF			
ROI mean ADC	0.76 ± 0.03	0.82 ± 0.03	.002[a]
ROI mean FA	0.53 ± 0.04	0.45 ± 0.07	.018[a]
Tract mean ADC	0.78 ± 0.03	0.85 ± 0.05	.002[a]
Tract mean FA	0.51 ± 0.03	0.44 ± 0.06	.014[a]
All NAWM			
ROI mean ADC	0.73 ± 0.02	0.79 ± 0.04	.0020[a]
ROI mean FA	0.68 ± 0.02	0.61 ± 0.04	.0098[a]
Tract mean ADC	0.75 ± 0.03	0.81 ± 0.05	.0098[a]
Tract mean FA	0.61 ± 0.03	0.55 ± 0.03	.002[a]

Note:—SLF indicates superior longitudinal fascicle; IFOF, inferior fronto-occipital fascicle; UF, uncinate fascicle; NAWM, normal-appearing white matter; ADC, apparent diffusion co-efficient, $\times 10^{-3}$ mm^2/s.
[a] Statistically significant.

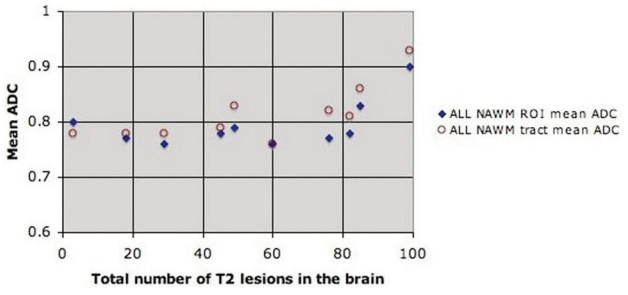

Fig 6. Scatterplots of the correlation between all NAWM regions of interest (ROIs) and tract-based mean ADC values of pediatric patients with MS compared with the total number of T2 lesions in the brain. Circles and diamonds represent the mean values.

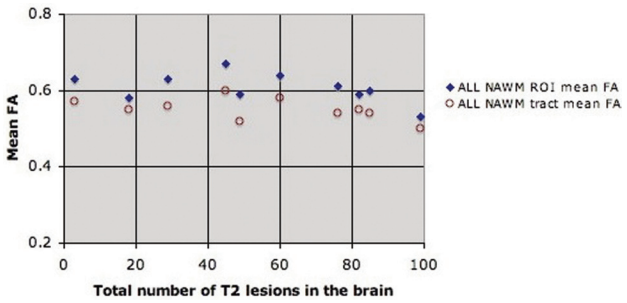

Fig 7. Scatterplots of the correlation between all NAWM ROIs and tract-based mean FA values of pediatric patients with MS compared with the total number of T2 lesions in the brain. Circles and diamonds represent the mean values.

The total number of lesions in the entire brain ranged from 3 to 99. The total number of T2 lesions in the brain significantly correlated with tract-based mean ADC of fibers passing through all NAWM (Fig 6) (Spearman correlation coefficient = 0.73, *P* value = .017). There was a trend toward a linear correlation with ROI mean ADC of all NAWM, but this trend failed to meet statistical significance (Spearman correlation coefficient = 0.40, *P* value = .26). In addition, a trend toward linear correlation with the ROI mean FA of all NAWM (Fig 7) (Spearman correlation coefficient = 0.39, *P* value = .26) and the tract-based mean FA of all NAWM (Spearman correlation coefficient = 0.59, *P* value = 0.072) was observed with the total number of T2 lesions in the brain, but the relationships failed to meet statistical significance, perhaps due to the limited sample size.

Discussion

The main objective of this preliminary study was to assess the DTI and tract-based DTI measures in 3 major white matter

pathways in pediatric patients with MS. In summary, we have found that ROI mean ADC in the midline CC, PLIC, and LAF was significantly higher and mean FA was significantly lower in pediatric patients with MS compared with normative controls. ROI analysis of NAWM in pediatric patients with MS showed the mean ADC to be higher and the mean FA to be lower except for the genu of the CC, PLIC, and CP. However, the tract-based mean ADC for all the fibers passing through NAWM was significantly higher, and the mean FA was significantly lower in children with MS. There was no significant association between ROI or tract-based FA and total T2 lesion load.

Consistent with studies in adult MS,[33-35] we found diffusion abnormalities in ROIs placed in the midline CC, PLIC, and LAF in patients with pediatric MS. Coombs et al[35] demonstrated increased mean ADC and decreased mean FA in the entire CC of adult patients with MS (Table 1), which mimic our findings. In our pediatric cohort, we also found elevated ADC and decreased mean FA in the callosal, projection, and LAF systems (Table 1), in agreement with prior DTI tractography studies in adult patients with MS,[20-24] suggesting that tract-based abnormalities are present regardless of age of onset.

DTI-based tractography provides an opportunity for further study of the connectivity and function of these white matter pathways.[19] Similar to findings in our pediatric MS study, tractography studies[22-24] in adult patients with MS have demonstrated significant involvement of the callosal fiber system, corticospinal tracts, and association fiber systems, correlating with cognitive dysfunction and motor disability. Lin et al[20] demonstrated significant increase in the mean ADC along the corticospinal tracts[23] and the corpus callosum[22] of adult patients with MS, correlating with disability by using the pyramidal functional status score and the Paced Auditory Serial Addition Test scores, which are used to assess cognitive function in MS.

In our study, we also found significant involvement of the association fiber system in pediatric patients with MS in agreement with adult MS studies.[21,24] These fibers are thought to be involved in the relay of information regarding spatial awareness, recognition, memory, visual perception, and other cognitive functions that are still under extensive research.[36-38] Studies of the involvement of these fibers may provide more insight into the mechanisms of cognitive dysfunction that are frequently observed in pediatric patients with MS.[39,40] In this preliminary study, we grouped the right and left LAF together (Fig 3*B*). Future larger studies may isolate left and right systems to correlate involvement with functional assessments. Overall, our findings demonstrate a similar extent of tract involvement in pediatric MS compared with published studies in the adult MS population, suggesting that the underlying pathophysiology of disease does not vary with age. However, larger comparative studies are needed to validate this hypothesis.

The total T2 lesion burden in pediatric patients with MS correlated with tract mean ADC of all NAWM tracts (Fig 6) and mean FA (Fig 7), though statistically insignificant. The lack of statistical significance may be due to small numbers, low lesion activity, and shorter disease duration observed in our cohort compared with adult MS studies.[18]

It is increasingly recognized that NAWM is affected in adult MS.[15-18] Similar to authors of studies in adult MS,[17,34,41] we found that children with MS had higher mean ADC and decreased mean FA in ROIs used to segment NAWM (Table 2). The CC appears to be a commonly affected area in MS both when normal-appearing and lesioned CC were examined.[18,23,34] In agreement with authors of these studies of adult patients with MS, we found a significant increase in the mean ADC and a decrease in the mean FA in the normal-appearing ROIs for the splenium of the CC of pediatric patients with MS and did not find any significance in the mean FA of ROIs for the normal-appearing genu of the CC and PLIC. In contrast to findings of authors of adult MS studies,[18] we found significantly increased mean ADC in the ROIs for a normal-appearing genu of the CC, PLIC, and CP in the pediatric patients with MS, compared with normative controls. Further comparative studies are necessary to determine whether there is selective vulnerability in the genu of the corpus callosum and descending pathways in pediatric-onset MS compared with adult-onset MS. Our results demonstrate increased mean ADC in the ROIs of NAWM as well as tracts passing through NAWM in pediatric patients with MS, suggesting that diffuse damage is present even in early-onset MS. Most of our patients were within 2 years of disease onset, supporting the notion that diffuse damage and neurodegenerative mechanisms are present from very early in the disease course. Further studies are required to confirm these findings.

To our knowledge, our study is the first published report investigating tract-based diffusion abnormalities in pediatric MS. The main limitations of this study are the small sample size, retrospective nature, and variable DTI techniques. However, we have tried to overcome this last limitation by using controls matched for scanner subtype and DTI acquisition techniques. Future studies will focus on using higher resolution uniform DTI to isolate and study diffusion parameters of functionally specific white matter tracts and on correlating these tract-based measures with clinical and neuropsychological manifestations of pediatric MS.

Conclusions

In summary, our findings—that is, ROI and tract-based abnormalities in white matter–containing lesioned and nonlesioned pathways and in the NAWM not containing lesioned pathways are both affected—suggest that there is diffuse damage evident in the early stages of pediatric MS, pointing to the need for early treatment intervention. The early detection of DTI abnormalities suggests that DTI has a strong potential to serve as an outcome measure in clinical trials. Given the sensitivity of the tract-based measures shown in this study combined with the potential to associate specific cognitive tasks with the tract-based measures, DTI may be particularly useful in assessing the impact of MS on specific neurologic functions. Future studies need to involve large prospective cohorts to validate the involvement of major white matter structures in pediatric patients with MS in correlation with functional assessment. Such future studies will greatly improve our understanding of the extent of deficits in children with MS as well as the temporal evolution and impact on physical and cognitive function.

References

1. Chitnis T. **Pediatric multiple sclerosis.** *Neurologist* 2006;12:299–310
2. Chitnis T, Glanz B, Jaffin S, et al. **Demographics of pediatric-onset multiple sclerosis in an MS center population from the Northeastern United States**. *Mult Scler* 2009;15:627–31. Epub 2009 Mar 19
3. Boiko A, Vorobeychik G, Paty D, et al. **Early-onset multiple sclerosis: a longitudinal study.** *Neurology* 2002;59:1006–10
4. Simone IL, Carrara D, Tortorella C, et al. **Course and prognosis in early-onset MS: comparison with adult-onset forms.** *Neurology* 2002;59:1922–28
5. MacAllister WS, Belman AL, Milazzo M, et al. **Cognitive functioning in children and adolescents with multiple sclerosis.** *Neurology* 2005;64:1422–25
6. Krupp LB, Banwell B, Tenembaum S. **Consensus definitions proposed for pediatric multiple sclerosis and related disorders.** *Neurology* 2007;68:S7–12
7. Gorman MP, Healy BC, Polgar-Turcsanyi M, et al. **Increased relapse rate in pediatric-onset compared with adult-onset multiple sclerosis.** *Arch Neurol* 2009;66:54–59
8. Trapp BD, Peterson J, Ransohoff RM, et al. **Axonal transection in the lesions of multiple sclerosis.** *N Engl J Med* 1998;338:278–85
9. Kutzelnigg A, Lucchinetti CF, Stadelmann C, et al. **Cortical demyelination and diffuse white matter injury in multiple sclerosis.** *Brain* 2005;128:2705–12
10. Gallo A, Rovaris M, Riva R, et al. **Diffusion-tensor magnetic resonance imaging detects normal-appearing white matter damage unrelated to short-term disease activity in patients at the earliest clinical stage of multiple sclerosis.** *Arch Neurol* 2005;62:803–08
11. Hahn CD, Shroff MM, Blaser SI, et al. **MRI criteria for multiple sclerosis: evaluation in a pediatric cohort.** *Neurology* 2004;62:806–08
12. Le Bihan D, Mangin JF, Poupon C, et al. **Diffusion tensor imaging: concepts and applications.** *J Magn Reson Imaging* 2001;13:534–46
13. Basser PJ, Pierpaoli C. **Microstructural and physiological features of tissues elucidated by quantitative-diffusion-tensor MRI.** *J Magn Reson B* 1996;111:209–19
14. Pierpaoli C, Jezzard P, Basser PJ, et al. **Diffusion tensor MR imaging of the human brain.** *Radiology* 1996;201:637–48
15. Cassol E, Ranjeva JP, Ibarrola D, et al. **Diffusion tensor imaging in multiple sclerosis: a tool for monitoring changes in normal-appearing white matter.** *Mult Scler* 2004;10:188–96
16. Werring DJ, Clark CA, Barker GJ, et al. **Diffusion tensor imaging of lesions and normal-appearing white matter in multiple sclerosis.** *Neurology* 1999;52:1626–32
17. Ciccarelli O, Werring DJ, Barker GJ, et al. **A study of the mechanisms of normal-appearing white matter damage in multiple sclerosis using diffusion tensor imaging–evidence of Wallerian degeneration.** *J Neurol* 2003;250:287–92
18. Ciccarelli O, Werring DJ, Wheeler-Kingshott CA, et al. **Investigation of MS normal-appearing brain using diffusion tensor MRI with clinical correlations.** *Neurology* 2001;56:926–33
19. Basser PJ, Pajevic S, Pierpaoli C, et al. **In vivo fiber tractography using DT-MRI data.** *Magn Reson Med* 2000;44:625–32
20. Lin F, Yu C, Jiang T, et al. **Diffusion tensor tractography-based group mapping of the pyramidal tract in relapsing-remitting multiple sclerosis patients.** *AJNR Am J Neuroradiol* 2007;28:278–82
21. Rocca MA, Pagani E, Absinta M, et al. **Altered functional and structural connectivities in patients with MS: a 3-T study.** *Neurology* 2007;69:2136–45
22. Lin X, Tench CR, Morgan PS, et al. **Use of combined conventional and quantitative MRI to quantify pathology related to cognitive impairment in multiple sclerosis.** *J Neurol Neurosurg Psychiatry* 2008;79:437–41
23. Hasan KM, Gupta RK, Santos RM, et al. **Diffusion tensor fractional anisotropy of the normal-appearing seven segments of the corpus callosum in healthy adults and relapsing-remitting multiple sclerosis patients.** *J Magn Reson Imaging* 2005;21:735–43
24. Rocca MA, Valsasina P, Ceccarelli A, et al. **Structural and functional MRI correlates of Stroop control in benign MS.** *Hum Brain Mapp* 2009;30:276–90
25. Wilson M, Tench CR, Morgan PS, et al. **Pyramidal tract mapping by diffusion tensor magnetic resonance imaging in multiple sclerosis: improving correlations with disability.** *J Neurol Neurosurg Psychiatry* 2003;74:203–07
26. Mezzapesa DM, Rocca MA, Falini A, et al. **A preliminary diffusion tensor and magnetization transfer magnetic resonance imaging study of early-onset multiple sclerosis.** *Arch Neurol* 2004;61:366–68
27. Tortorella P, Rocca MA, Mezzapesa DM, et al. **MRI quantification of gray and white matter damage in patients with early-onset multiple sclerosis.** *J Neurol* 2006;253:903–07
28. Mori S, van Zijl PC. **Fiber tracking: principles and strategies—a technical review.** *NMR Biomed* 2002;15:468–80
29. Wakana S, Jiang H, Nagae-Poetscher LM, et al. **Fiber tract-based atlas of human white matter anatomy.** *Radiology* 2004;230:77–87
30. Catani M, Howard RJ, Pajevic S, et al. **Virtual in vivo interactive dissection of white matter fasciculi in the human brain.** *Neuroimage* 2002;17:77–94
31. Catani M, Thiebaut de Schotten M. **A diffusion tensor imaging tractography atlas for virtual in vivo dissections.** *Cortex* 2008;44:1105–32. Epub 2008 May 23
32. Mamata H, Mamata Y, Westin CF, et al. **High-resolution line scan diffusion tensor MR imaging of white matter fiber tract anatomy.** *AJNR Am J Neuroradiol* 2002;23:67–75
33. Yu CS, Zhu CZ, Li KC, et al. **Relapsing neuromyelitis optica and relapsing-remitting multiple sclerosis: differentiation at diffusion-tensor MR imaging of corpus callosum.** *Radiology* 2007;244:249–56
34. Rueda F, Hygino LC Jr, Domingues RC, et al. **Diffusion tensor MR imaging evaluation of the corpus callosum of patients with multiple sclerosis.** *Arq Neuropsiquiatr* 2008;66:449–53
35. Coombs BD, Best A, Brown MS, et al. **Multiple sclerosis pathology in the normal and abnormal appearing white matter of the corpus callosum by diffusion tensor imaging.** *Mult Scler* 2004;10:392–97
36. Schmahmann JD, Pandya DN, Wang R, et al. **Association fibre pathways of the brain: parallel observations from diffusion spectrum imaging and autoradiography.** *Brain* 2007;130(Pt 3):630–53. Epub 2007 Feb 9
37. Turken A, Whitfield-Gabrieli S, Bammer R, et al. **Cognitive processing speed and the structure of white matter pathways: convergent evidence from normal variation and lesion studies.** *Neuroimage* 2008;42:1032–44
38. Urbanski M, Thiebaut de Schotten M, Rodrigo S, et al. **Brain networks of spatial awareness: evidence from diffusion tensor imaging tractography.** *J Neurol Neurosurg Psychiatry* 2008;79:598–601
39. MacAllister WS, Christodoulou C, Milazzo M, et al. **Longitudinal neuropsychological assessment in pediatric multiple sclerosis.** *Dev Neuropsychol* 2007;32:625–44
40. Amato MP, Goretti B, Ghezzi A, et al. **Cognitive and psychosocial features of childhood and juvenile MS.** *Neurology* 2008;70:1891–97
41. Ge Y, Law M, Johnson G, et al. **Preferential occult injury of corpus callosum in multiple sclerosis measured by diffusion tensor imaging.** *J Magn Reson Imaging* 2004;20:1–7
42. Makris N, Kennedy DN, McInerney S, et al. **Segmentation of subcomponents within the superior longitudinal fascicle in humans: a quantitative, in vivo, DT-MRI study.** *Cereb Cortex* 2005;15:854–69